



## Determining butanol inhibition kinetics on the growth of *Clostridium pasteurianum* based on continuous operation and pulse substrate additions

Kalafatakis, Stavros; Skiadas, Ioannis V.; Gavala, Hariklia N.

*Published in:*  
Journal of Chemical Technology and Biotechnology

*Link to article, DOI:*  
[10.1002/jctb.5919](https://doi.org/10.1002/jctb.5919)

*Publication date:*  
2019

*Document Version*  
Peer reviewed version

[Link back to DTU Orbit](#)

*Citation (APA):*  
Kalafatakis, S., Skiadas, I. V., & Gavala, H. N. (2019). Determining butanol inhibition kinetics on the growth of *Clostridium pasteurianum* based on continuous operation and pulse substrate additions. *Journal of Chemical Technology and Biotechnology*, 94(5), 1559-1566. <https://doi.org/10.1002/jctb.5919>

---

### General rights

Copyright and moral rights for the publications made accessible in the public portal are retained by the authors and/or other copyright owners and it is a condition of accessing publications that users recognise and abide by the legal requirements associated with these rights.

- Users may download and print one copy of any publication from the public portal for the purpose of private study or research.
- You may not further distribute the material or use it for any profit-making activity or commercial gain
- You may freely distribute the URL identifying the publication in the public portal

If you believe that this document breaches copyright please contact us providing details, and we will remove access to the work immediately and investigate your claim.

Determining butanol inhibition kinetics on the growth of  
*Clostridium pasteurianum* based on continuous operation  
and pulse substrate additions

Stavros Kalafatakis, Ioannis V. Skiadas, Hariklia N. Gavala\*

Technical University of Denmark (DTU), Department of Chemical and Biochemical  
Engineering, Søtofts Plads 229, 2800 Kgs. Lyngby, Denmark.

\*Corresponding author: e-mail: [hnga@kt.dtu.dk](mailto:hnga@kt.dtu.dk) & [hari\\_gavala@yahoo.com](mailto:hari_gavala@yahoo.com) tel:

+4545256196

**Short running title:** Determining inhibition kinetics

This article has been accepted for publication and undergone full peer review but has not been through the copyediting, typesetting, pagination and proofreading process which may lead to differences between this version and the Version of Record. Please cite this article as doi: 10.1002/jctb.5919

## Abstract

**BACKGROUND:** *Clostridium pasteurianum* is a well described strain for the conversion of glycerol into butanol. In general, cell growth kinetics depends on the type of glycerol used and the concentration of butanol in the fermentation broth. However, despite the numerous studies existing on the subject, there is limited information in the literature regarding growth inhibition kinetics due to the cytotoxic effect of butanol on the cell growth. This can be attributed to the difficulty of growing cells at high butanol concentration which renders the determination of inhibition kinetics a rather challenging task.

**RESULTS:** During this study a new approach for the determination of the butanol inhibition kinetics on the growth of *C. pasteurianum* was tested. Specifically, pulses of crude glycerol were applied when steady state was reached during continuous fermentation experiments with increasing butanol concentration in the feed. Combining pulse experiments with batch fermentation at low substrate concentration allowed for accurate determination of the kinetic constants for inhibited growth. This approach also minimised the correlation of the growth constants which often leads to poor identifiability.

**CONCLUSION:** In overall, the proposed experimental approach showed good identifiability of the kinetic parameters for butanol inhibition of the microbial growth and can be proven valuable for the determination of inhibitory effects of highly toxic compounds.

**Keywords:** *C. pasteurianum*, butanol inhibition, crude glycerol, fermentation, kinetics and modeling

Accepted Article

## INTRODUCTION

The rapid growth of biodiesel industry has generated a large surplus of crude glycerol in amounts corresponding approximately to one-tenth of total biodiesel production.<sup>1,2</sup> Purified glycerol has numerous applications in the chemical industry, ranging from food products to soaps.<sup>3</sup> Furthermore, microbes of the *Lactobacillus*, *Klebsiella* and *Clostridium* genus have been reported to convert glycerol to mainly 1,3-PDO, butanol, ethanol, butyric acid, acetate and others.<sup>4-9</sup> Whereas substrate inhibition during pure glycerol fermentation is observed only in very high concentrations, cell proliferation in moderate or even low crude glycerol concentrations was proven challenging.<sup>10-12</sup> The latter can be attributed to impurities that are found in the crude glycerol solution and can hinder bacterial growth. Namely, methanol, salts and unsaturated fatty acids have been reported to delay or even seize bacterial growth.<sup>13-16</sup> Nevertheless, crude glycerol composition and consequently the intensity of microbial growth inhibition depend on i) the feedstock used (1<sup>st</sup> or 2<sup>nd</sup> generation oils and fats) and ii) the processing applied for the biodiesel production and therefore can vary considerably. A typical crude glycerol composition derived from biodiesel industry using vegetable oil corresponds to: 62.5-76.6% glycerol, 75-83% carbohydrates, 0.06-0.44 protein, 1-13% fat, 0.25-2.8% ash and 3.17-3.86% residual methanol<sup>17</sup>, while crude glycerol composition derived from animal fat based biodiesel is: 75 % glycerol, 10 % fat, 1-2% sulphur, 10 % water, 5 % ash and <1 % methanol.<sup>18</sup> Microbial adaptation and/or feedstock purification are common practices applied for alleviating any bacterial growth inhibition during crude glycerol fermentation.<sup>14,18-21</sup> Additionally, the fermentation products and especially alcohols can hinder bacterial growth, thus reducing product yields and production rates. Namely, butanol concentrations

Accepted Article

corresponding to  $17 \text{ g L}^{-1}$ <sup>22</sup> and  $12.3 \text{ g L}^{-1}$ <sup>23</sup> were reported when pure and crude glycerol (after mild physical pre-treatment) were used as carbon source during *C. pasteurianum* fermentation, respectively (without product removal). To the best of our knowledge the highest butanol concentration recorded for *C. pasteurianum* was  $21 \text{ g L}^{-1}$  during mixed carbon source fermentation (1:1 glucose/glycerol).<sup>24</sup> Generally, 1-2% of butanol is reported to be inhibitory for a wide range of microorganisms, whereas some *Lactobacillus* strains can tolerate butanol concentrations up to 3%.<sup>25</sup> Furthermore, later studies demonstrated that butanol has an acute cytotoxic effect on the cells, whereas ethanol has a milder reversible cytostatic influence.<sup>26</sup> Specifically for *Clostridium acetobutylicum* it has been reported that  $15 \text{ g L}^{-1}$  of butanol reduces 3-fold the cell formation whereas 20-25  $\text{g L}^{-1}$  totally inhibited growth.<sup>27</sup> Also, Venkataramanan and colleagues (2014) studied the effect of membrane conformational changes under butanol inhibition conditions and reported that the optical density of fully grown cultures was reduced even after the addition of  $2.5 \text{ g L}^{-1}$  of butanol.<sup>28</sup> Despite the numerous studies on butanol production found in the literature and the well-known highly inhibitory effect of butanol on cell growth there is a lack of studies addressing inhibition kinetics, also revealed by the review of Mayank et al. on modeling of ABE fermentation.<sup>29</sup> Traditionally, microbial inhibition kinetics are determined through a series of batch experiments at elevated concentration of the inhibitory compound by monitoring the rate of microbial biomass growth and substrate consumption.<sup>15,30,31</sup> However, this methodology can be hardly applied in cases of intense inhibition as this might cause irregular and very long lag-phases, especially when sporulating microorganisms are used. Moreover, determining the microbial growth kinetics on a highly inhibitory feedstock, like crude

glycerol can be equally challenging.<sup>11,12</sup> In order to increase the sensitivity of the simultaneous determination of the maximum specific growth rate and saturation constant, batch experiments at increasing initial substrate concentrations is the commonly applied method.<sup>32</sup> However, this can also lead to substrate inhibition and/or irregular and long lag phases, as in the case above, depending on the intensity of substrate inhibition.

In the current study, a different experimental approach was followed. The effect of butanol on the growth kinetics of *C. pasteurianum* was assessed in continuous cultures with increasing butanol concentration and pulses of crude glycerol when a steady state was reached. The amount of crude glycerol injected in the reactor was regulated in a way that allowed monitoring of glycerol consumption while securing that no inhibition due to the feedstock occurred. The sensitivity of simultaneous determination of the kinetic constants was increased by fitting the data from the continuous experiments together with the data from a batch experiment. Thus, accurate determination of kinetic parameters of butanol inhibition kinetics on *C. pasteurianum* growth was possible. Growth kinetics determination through continuous experiments and substrate spikes have been reported before<sup>33-35</sup>, however and to our knowledge, this is the first time that such a methodology has been applied for determining inhibition kinetics combining increasing influent concentration of the inhibitor and substrate pulses. The methodology applied here can have ample applications in determining microbial growth and inhibition kinetics when highly inhibitory substances/matrices are involved.

## MATERIALS AND METHODS

### Bacterial strain and freeze stock preparation

*Clostridium pasteurianum*, strain DSM 525 was purchased as freeze dried powder from the German Collection of Microorganism and cell cultures (DSMZ, Göttingen, Germany). The cells were activated in sterile anaerobically prepared medium 54b (glucose 20.0 g L<sup>-1</sup>; yeast extract 10.0 g L<sup>-1</sup>, CaCO<sub>3</sub> 20 g L<sup>-1</sup>), and incubated overnight at 37°C, under continuous agitation (150 rpm). After minor adaptation (two consecutive transfers), 10% (v/v) fully grown cultures were transferred with a syringe in a sterile medium described by from Biebl (2001), supplemented with FeSO<sub>4</sub> (7.5 mg L<sup>-1</sup>)<sup>36</sup> and 10 g L<sup>-1</sup> pure glycerol (Sigma, St. Louis, Missouri, USA). Freeze stocks were kept in anaerobic and sterile glass vials at – 80°C supplemented with pure glycerol solution (10% w/w final concentration) (Sigma, St. Louis, Missouri, USA). Prior each experiment a new freeze stock culture was activated.

### Pre-treatment of crude glycerol

A modified protocol described elsewhere<sup>21</sup> was used for the treatment of crude glycerol (provided by DAKA ecoMotion, Løsning, Denmark). The composition of crude glycerol used in the present study is described in Varrone et al.<sup>18</sup> In short: i) pH was adjusted to 6.0 with KOH (Sigma-Aldrich, St. Louis, Missouri, USA) pellets, ii) solid particles were removed by centrifugation at 4400 rpm for 15 min, iii) anhydrous 95% n-hexane (Sigma-Aldrich, St. Louis, Missouri, USA) and pH 6.0 crude glycerol were mixed in ratio 1:1 for 3 h at 200 rpm; iv) phase separation took place in 2 L separation funnel for 1.5 h, v) the lower phase was retained and vi) steps ii-v were repeated. Hexane treatment was applied in order to remove



inhibiting amounts of Long Chain Fatty Acids from crude glycerol, which may negatively interfere with the membrane of Gram-positive microbial strains. After treatment, approximately 137 g COD/L was removed from crude glycerol as reported in Varrone et al.<sup>18</sup>

## **Fermentations**

### ***Batch fermentation without pH control***

Batch fermentations were performed at 37°C, under 150 rpm agitation, in 117 mL serum vials with 50 mL working volume (10% v/v inoculum). Also, NaHCO<sub>3</sub> (2.6 g L<sup>-1</sup>) (Sigma-Aldrich, St. Louis, Missouri, USA) was supplemented for pH maintenance ~6.0. Carbon source was either pure glycerol (Sigma-Aldrich, St. Louis, Missouri, USA), or crude glycerol/hexane treated glycerol (Daka ecoMotion A/S, Løsning, Denmark).

### ***Reactor fermentation - Batch and continuous fermentations***

Reactor fermentations were performed in a 3-L glass reactor (Applikon<sup>®</sup>, Delft, the Netherlands) and fermentation volume was set to 1 L. Temperature (37°C), agitation (200 rpm) and pH 6.0 (4M KOH solution, Sigma-Aldrich, St. Louis, Missouri, USA) were controlled with an ez-control unit (Applikon<sup>®</sup>, Delft, the Netherlands). Modified Biebl (2001) medium (as described in “Bacterial strain and freeze stock preparation” section), supplemented with approximately 10 g L<sup>-1</sup> hexane treated crude glycerol and 30 µL of Antifoam 204 (Sigma-Aldrich, St. Louis, Missouri, USA) per litre of medium was used. Batch fermentations initiated with the inoculation of 50 mL (5% v/v) pre-culture in mid-late exponential phase (OD<sub>600</sub>=1.2-1.4). For the continuous fermentation the hydraulic retention time was 14.25 h. Steady state was considered after a minimum of 5-6 hydraulic retention

Accepted Article

times in combination to stable cell concentration and gas production. For the fermentation influent, 10 L growth medium batches (same composition to the batch) were prepared, autoclaved at 121°C for 40 min and consecutively gassed through a sterile gas PTFE filters (0.20 µm pore size, Midistart<sup>®</sup>, Sartorius, Ireland) with nitrogen 99.9% for 1.5 h. Finally, 1-butanol (purity 99%, Sigma-Aldrich, St. Louis, Missouri, USA) was supplemented after sparging and mixed with a magnetic stirrer until a homogenous mixture was acquired. The feed solution kept at 4°C to minimize possible contamination and substrate consumption. The concentration of butanol and glycerol for each growth media used for the continuous fermentation were determined both at the beginning and the end of the feeding process. Substrate, cells and products concentration including H<sub>2</sub> was monitored throughout the duration of the experiments.

During the continuous experimentation, in total there were 5 steady states reached at 0 (0-140 h), 1 (140-330 h), 2 (330-470 h), 3 (470-640 h) and 4 g/L (640-780 h) butanol concentration in the influent (with ~ 10 g/L glycerol influent concentration) and three glycerol pulses were imposed during the 1<sup>st</sup>, 3<sup>rd</sup> and 4<sup>th</sup> steady state as described in the sequel. The variability of all main metabolites at steady state was less than 10%.

### **Pulse experiments**

A concentrated solution (100 g L<sup>-1</sup>) of hexane treated crude glycerol was pulse-fed during different steady states and consecutively the substrate concentration was monitored for 5 h. The pulse-fed solution was prepared anaerobically in Biebl (2001) medium reaching a final

Accepted Article

volume of 20 mL and the glycerol concentration into the reactor after the perturbation reached 2 g L<sup>-1</sup>. The final concentration of the pulse-fed glycerol was kept low in order to minimize substrate inhibition effects.

### **Analytical methods**

Glycerol and fermentation products quantification was performed via High Performance Liquid Chromatography (HPLC) equipped with an Aminex HPX-87H column (Bio-Rad, Hercules, California, USA) and a refractive index detector. Separation was performed at 0.6 mL min<sup>-1</sup> flowrate with a H<sub>2</sub>SO<sub>4</sub> solution (12 mM, Sigma-Aldrich, St. Louis, Missouri, USA). Hydrogen was quantified by 0.2 mL injections to a Mikrolab gas chromatography (Mikrolab Aarhus, Højbjerg, Denmark) equipped with a thermal conductivity detector and a Porapack Q column (Agilent Technologies, Santa Clara, USA): Oven, injection and detector temperatures were set at 70°C and pure nitrogen was used as carrier gas at a 50 mL min<sup>-1</sup> flowrate. Finally, microbial biomass was quantified via a Total Suspended Solids/OD<sub>600</sub> calibration curve (linearly correlated, see “Calibration curve” section). Total Suspended Solids were measured according to the method described at “Standard methods for examination of water and wastewater”<sup>37</sup> with Whatman<sup>TM</sup> glass microfiber filters, 0.7 μm particle retention (GE Healthcare Europe GmbH, Denmark).

### **Modeling microbial growth and inhibition kinetics**

Microbial growth and substrate consumption were modeled according to equations 1 and 2, respectively. Monod kinetics with first order decay was applied for non-inhibited growth,

while the inhibition function,  $I_{but}$ , referring to uncompetitive inhibition<sup>38</sup> by butanol, was assumed and modeled according to equation 3.

$$\frac{dX}{dt} = \frac{\mu_{max} \cdot S}{K_S + S} \cdot X \cdot I_{but}^2 - k_d \cdot X \quad (1)$$

$$\frac{dS}{dt} = \frac{1}{Y_{X/S}} \cdot \frac{\mu_{max} \cdot S}{K_S + S} \cdot X \cdot I_{but}^2 \quad (2)$$

Where  $\mu_{max}$  is the maximum specific growth rate ( $h^{-1}$ ),  $K_S$  is the saturation constant ( $g L^{-1}$ ),  $K_d$  is the decay constant ( $h^{-1}$ ),  $Y_{X/S}$  is the microbial cells yield ( $g \text{ cells} / g \text{ glycerol}$ ),  $S$  and  $X$  is the substrate (glycerol) and microbial cells concentration ( $g L^{-1}$ ), respectively, and  $I_{but}$  is the butanol inhibition function.

$$I_{but} = \frac{K_I}{K_I + I} \quad (3)$$

Where  $K_I$  is the inhibition constant ( $h^{-1}$ ) and  $I$  is the concentration of the inhibitor ( $g L^{-1}$ ), which is butanol in this study.

Butanol production from glycerol during fermentation by *C. pasteurianum* was simulated according to equation 4:

$$\frac{dP}{dt} = \frac{Y_{P/S}}{Y_{X/S}} \cdot \frac{\mu_{max} \cdot S}{K_S + S} \cdot X \cdot I_{but}^2 \quad (4)$$

Where  $P$  is the product, butanol, concentration ( $g L^{-1}$ ) and  $Y_{P/S}$  is the yield of butanol per substrate ( $g \text{ butanol} / g \text{ glycerol}$ ).

In order to estimate the kinetic constants ( $\mu_{max}$ ,  $K_S$ ,  $K_I$ , and  $k_d$ ), equations 1-4 were used for simultaneously fitting the data for glycerol, butanol and cells concentration obtained from the batch experiment in the fermentor and the continuous experiments (including glycerol pulses), as described in the “Fermentations” section, using the computer software “Aqsim 2.0”.<sup>39</sup>

The kinetic constants were estimated by minimizing the sum of the squares ( $x^2(p)$ ) of the weighted deviations between measurements and calculated model results according to equation 5:

$$x^2(p) = \sum_{i=1}^n \left( \frac{y_{meas,i} - y_i(p)}{\sigma_{meas,i}} \right)^2 \quad (5)$$

Where  $y_{meas,i}$  and  $y_i$  were the measured and predicted by the model values of state variables (namely the concentrations of the glycerol, cells and butanol) and  $\tilde{A}_{meas,i}$  was the standard deviation for each measured entity. The secant algorithm was used for the parameters estimation and therefore the standard deviation for each estimated value of kinetic constants was calculated as well.

Identifiability of the estimated constants was performed using the absolute-relative sensitivity function of Aqsim,  $\delta_{y,p}^{\alpha,r}$ , which measures the absolute change of the state variables (in this case, glycerol, butanol and cells concentration) per unit of change of the model constants as given by equation 6.

$$\delta_{y,p}^{\alpha,r} = p \cdot \frac{\partial y}{\partial p} \quad (6)$$

Where  $y$  denotes the state variables and  $p$  the constants of the model.

### **Electron balances and stoichiometric analysis**

Complete stoichiometric equations were extracted based on electron balance between the measured substrate consumption and metabolites and cells production according to the method reported in Rittmann and McCarty.<sup>38</sup> In short, this approach is based on considering the carbon substrate in fermentation processes also as electron pool, a fraction of which is directed towards the “energy” generating catabolic reactions while the rest is used for biomass synthesis through the energy consuming anabolic reactions. According to this, stoichiometric equations were first set-up taking into account the amount of glycerol consumed and all metabolites (except cells) produced. Subsequently the fraction of electrons of the substrate that was directed to products ( $f_e$ ) was quantified based on the ratio of the actual yield to the theoretical yield predicted by the stoichiometric coefficient. The remaining fraction of electrons of the substrate that were not found in the metabolites ( $f_s = 1 - f_e$ ) was assigned to cells growth and the overall stoichiometric equation was extracted. It is important to mention that since the maintenance requirements of the cells in general vary depending on the fermentation conditions, the actual yield of cells was always lower than the theoretically predicted; therefore the difference between the theoretical ( $f_s$ ) and experimental cells yield ( $f_{s,exp}$ ) was used to extract conclusions regarding the electron fraction of the substrate used for maintenance energy requirements ( $f_m = f_s - f_{s,exp}$ ).

## RESULTS AND DISCUSSION

### Batch fermentations with crude glycerol and hexane treated crude glycerol

Initial experiments performed with non-treated crude glycerol showed long lag phases (3-4 days) even at low,  $10 \text{ g L}^{-1}$ , substrate concentrations and therefore, pre-treatment of crude glycerol with hexane was performed. Fermentation with hexane treated crude glycerol showed shorter lag phase and better growth consistency at  $10 \text{ g L}^{-1}$  substrate concentration (see **Figure 1A & Figure 1B**). In fact, hexane-treated crude glycerol performed equally well with pure glycerol and the small measured difference in the final cells concentration (measured as TSS, Figure 1B) was due to the different initial glycerol concentration ( $12.8 \text{ g/L}$  pure glycerol compared to  $10.8 \text{ g/L}$  glycerol in hexane-treated crude glycerol). Nevertheless, when the substrate concentration was increased or when butanol was supplemented in the growth medium prior the inoculation, the same issue of long lag phase or no growth at all was observed. When 1-butanol was added in the growth medium, prior inoculation, it was found to be inhibitory for bacterial growth at concentrations as low as  $2 \text{ g L}^{-1}$ . Those results confirmed the highly inhibitory effect of externally added butanol in cultures of *C. pasteurianum* that have been previously reported. Specifically, Venkataramanan and colleagues (2014) reported reduction of *C. pasteurianum* biomass even when  $2.5 \text{ g L}^{-1}$  of n-butanol was added in fully grown cultures.<sup>28</sup> Thus neither the main kinetic parameters ( $\mu_{max}$  and  $K_s$ ) nor the butanol inhibition constant,  $K_I$ , could be determined through batch experiments. Therefore and as it has been already mentioned, continuous fermentation and substrate pulse-feeding experiments were performed in an effort to alleviate the abovementioned challenges.

## Modelling reactor fermentations

### *Calibration curve*

The microbial growth was monitored by measuring the optical density, OD, of the fermentation broth at 600 nm. The mass of the cells for modeling purposes was then calculated using a calibration curve of the cells measured as Total Suspended Solids, TSS, versus OD. The calibration curve for *C. pasteurianum* is shown in **Figure 2**.

### *Modeling of butanol inhibition*

The fitting of the model to the experimental concentration of glycerol, butanol and cells in CSTR and batch is shown in **Figure 3 (A, B and C)**, **Figure 4 (A and B)** and **Figure 5 (A and B)**, respectively.

**Table 1** shows the values of the estimated constants together with their estimated standard deviation while the correlation matrix of the model constants is presented in **Table 2**. It is noticeable that all constants were estimated with a relatively high precision and they also exhibited a low correlation allowing thus for accurate determination of the optimal values of the constants within the limits set. Specifically for the inhibition constant, which is on the focus of the present study, the identifiability analysis showed a high sensitivity of glycerol concentration with respect to inhibition constant  $K_I$ , especially during the pulses in continuous experiments with increasing butanol concentration in the influent of the reactor while the sensitivity of butanol and cells concentration was low to negligible, respectively. The corresponding curves for the sensitivity of the state variables of the model with respect to  $K_I$  are shown in **Figure 6A** for the CSTR and **Figure 6B** for the batch fermentations. It can



Accepted Article

be observed that in the 1<sup>st</sup> phase of continuous experiments, where the butanol concentration was zero, the value of the sensitivity function of glycerol concentration was also zero, namely negligible, while it was increasing with increasing influent butanol concentration and exhibited the highest values during the pulses.

Another important point is the accuracy of the simultaneous estimation of both  $\mu_{max}$  and  $K_S$ , which usually suffer by a large correlation (changes in calculated concentrations brought by one constant can be compensated by an appropriate change of the other one) and therefore non-identifiability.<sup>39</sup> When the uncompetitive inhibition function was added to the model then a high correlation was observed between  $\mu_{max}$  and  $K_I$  (-0.83) and  $K_S$  and  $K_I$  (0.81) when the data from the batch fermentation was fitted to the model. Simultaneous fitting of the data obtained in batch and continuous mode, coupled with the substrate pulses, have led to a noticeable reduction of the abovementioned correlation coefficients, to -0.42 and 0.57, respectively.

In the current study a  $\mu_{max}$  corresponding to  $0.60 \pm 0.08 \text{ h}^{-1}$  was estimated by the model, as shown in **Table 1**, which is slightly higher than the ones reported in literature. Namely,  $\mu_{max}$  values ranging from  $0.37 \text{ h}^{-1}$ <sup>22</sup>, to  $0.31 \pm 0.01 \text{ h}^{-1}$  and  $0.23 \pm 0.01 \text{ h}^{-1}$  under iron excess and limitation, respectively<sup>40</sup> have been reported. The difference in the  $\mu_{max}$  can be attributed to the higher fermentation temperature that applied in the current study (37°C) compared to the abovementioned studies (35°C). Although a temperature difference of 2°C might seem low, a 47% decrease of the  $\mu_{max}$  during batches of *C. butyricum* when the temperature was decreased from 37 to 35°C have been reported.<sup>41</sup> Also, the higher  $\mu_{max}$  might be also attributed to compounds that are present in the crude glycerol that can induce cell growth. Finally, during

dark fermentation of crude glycerol for hydrogen production with *C. pasteurianum*, a saturation constant equal to 2.43 g L<sup>-1</sup> has been reported.<sup>42</sup> This is two-fold higher than the 1.13 g L<sup>-1</sup> estimated in the current study and it denotes the increased affinity of *C. pasteurianum* DSM 525 to the specific crude glycerol used.

In general and as it has already been mentioned, there is scarcity of studies regarding the kinetic determination of butanol inhibition. A very interesting study by Costa and Moreira (1983) describes product inhibition of butyric acid, butanol, acetic acid, acetone and ethanol on *C. acetobutylicum*. Interestingly butyric acid exhibited the lowest concentration of inhibitor that reduced  $\mu_{max}$  by a factor of 2 corresponding to 6 g L<sup>-1</sup> followed by butanol at a value of 11 g L<sup>-1</sup>.<sup>43</sup> This value is higher than the 7.64 g L<sup>-1</sup> reported in the present study (the calculated  $K_I$  value reflects the concentration of inhibitor that reduces  $\mu_{max}$  by a factor of 2); this can be attributed to the lower butanol tolerance for *C. pasteurianum* when compared to *C. acetobutylicum* as supported by literature studies.<sup>27,28,43</sup>

### 3.3 Electron balances and stoichiometric analysis

**Table 3** presents the stoichiometric coefficients for the overall conversion of glycerol to products and cells by *C. pasteurianum* growth for the batch fermentation and the different steady states with increasing influent butanol concentration.  $f_e$  and  $f_s$  represent the fraction of electrons of the substrate directed to products and cell synthesis, respectively. As mentioned, the calculations were based on the actual experimentally determined yields of the metabolic products, which were used for calculating  $f_e$  while  $f_s$  was calculated based on equation 7.<sup>38</sup>

$$f_s = 1 - f_e \quad (7)$$

Accepted Article

It is noticeable that the butanol yield changed significantly among the different steady states and the batch operation. The highest butanol yield, 0.28 mol butanol / mol glycerol, was observed in batch, while it was gradually decreasing in CSTR with increasing butanol concentration; starting with a value of 0.20 at the 1<sup>st</sup> steady state with 1.7 g/l butanol and reaching a value of 0.17 at the 5<sup>th</sup> steady state with 5.5 g/l butanol. This implies that butanol presence affects negatively butanol yield with the excess electrons being directed to H<sub>2</sub> and other reduced products, namely 1,3 PDO in this case. Indeed, both metabolites exhibited higher yields in CSTR compared to batch fermentation while their yields were increasing further with increasing butanol concentration in CSTR.

The overall stoichiometric equation can hardly fit the actual cells yield, as part of the energy generated during catabolic reactions is used for maintenance and therefore is not directed to anabolic reactions and cell synthesis. Based on the difference of the theoretical (as predicted by the stoichiometric equation) to the experimental cells yields, the actual fraction of substrate electrons directed to cells synthesis ( $f_{s,exp}$ ) and the fraction of electrons directed to maintenance ( $f_m$ ) can be calculated and are also presented in **Table 3**. One can observe that  $f_s$  value was in general lower in the batch fermentation compared to the  $f_s$  values for the continuous experiments (with the only exception steady state 2). The higher  $f_s$  calculated for the continuous experiments were actually due to the increased maintenance energy requirements rather than to increased cell synthesis as implied by the higher  $f_m$  values. This can very well be correlated and attributed to butanol inhibition since the batch fermentation started at a butanol concentration of zero while the concentration of butanol during the 1<sup>st</sup> steady state of the CSTR was already 1.7 g L<sup>-1</sup>. It is also noticeable that the highest value of

$f_m$  was reached when the butanol concentration in the CSTR increased to 5.5 g L<sup>-1</sup> (5<sup>th</sup> steady state with 4 g L<sup>-1</sup> influent butanol concentration).

## CONCLUSIONS

A new approach for the determination of the kinetic parameters of *C. pasteurianum* growth on crude glycerol under butanol inhibition was applied based on continuous fermentations with increasing influent butanol concentration and pulse substrate addition at steady state.

The main contribution of this work can be summarized as following:

- Crude glycerol originated from 2<sup>nd</sup> generation biodiesel based on animal fat could support growth of *C. pasteurianum* at low concentrations and only after pre-treatment by hexane.
- Increased butanol concentrations resulted in reduced butanol yields.
- The applied methodology resulted in accurate determination of the growth and inhibition constants by allowing for experimenting at higher butanol concentrations and reducing the correlation of the model constants.
- The determined  $K_I$  supported the highly inhibitory effects of butanol to the growth of *C. pasteurianum* indicating that 7.64 g L<sup>-1</sup> butanol lowers the effective  $\mu_{max}$  by a factor of 2.
- The effect of butanol on increasing the maintenance energy requirements of the cell was demonstrated by applying electron balances and stoichiometric calculations.

## Acknowledgements

The authors gratefully acknowledge financial support from the European Commission (FP7 Grant Agreement no 613667; acronym: GRAIL), the Technical University of Denmark and Innovation Fund Denmark (IBISS: Industrial Biomimetic Sensing and Separation)

Accepted Article

## References

1. Santibáñez C, Varnero MT, Bustamante M. Residual Glycerol from Biodiesel Manufacturing, Waste or Potential Source of Bioenergy: A Review. *Chil J Agric Res.* **71**: 3, 469–75 (2011).
2. Marchetti JM, Miguel VU, Errazu a. F. Possible methods for biodiesel production. *Renew Sustain Energy Rev.* **11**: 6, 1300–11 (2007).
3. Quispe C a G, Coronado CJR, Carvalho J a. Glycerol: Production, consumption, prices, characterization and new trends in combustion. *Renew Sustain Energy Rev.* Elsevier, **27**: 475–93 (2013).
4. Bouvet OMM, Lenormand P, Ageron E, Grimont PAD. Taxonomic diversity of anaerobic glycerol dissimilation in the *Enterobacteriaceae*. *Res Microbiol.* **146**: 4, 279–90 (1995).
5. Homann T, Tag C, Biebl H, Deckwer WD, Schink B. Fermentation of glycerol to 1,3-propanediol by *Klebsiella* and *Citrobacter* strains. *Appl Microbiol Biotechnol.* **33**: 2, 121–6 (1990).
6. Nakas JP, Schaedle M, Parkinson CM, Coonley CE, Tanenbaum SW. System development for linked-fermentation production of solvents from algal biomass. *Appl Environ Microbiol.* **46**: 5, 1017–23 (1983).
7. Sobolov M, Smiley KL. Metabolism of glycerol by an acrolein-forming *Lactobacillus*. *J Bacteriol.* **79**: 261–6 (1960).
8. Yazdani SS, Gonzalez R. Anaerobic fermentation of glycerol: a path to economic viability for the biofuels industry. *Curr Opin Biotechnol.* **18**: 213–9 (2007).

9. da Silva GP, Mack M, Contiero J. Glycerol: A promising and abundant carbon source for industrial microbiology. *Biotechnol Adv*. Elsevier Inc., **27**: 1, 30–9 (2009).
10. Gallardo R, Alves M, Rodrigues LR. Modulation of crude glycerol fermentation by *Clostridium pasteurianum* DSM 525 towards the production of butanol. *Biomass and Bioenergy*. Elsevier Ltd, **71**: 134–43 (2014).
11. Jensen TO, Kvist T, Mikkelsen MJ, Christensen PV, Westermann P. Fermentation of crude glycerol from biodiesel production by *Clostridium pasteurianum*. *J Ind Microbiol Biotechnol*. **39**: 5, 709–17 (2012).
12. Taconi KA, Venkataramanan KP, Johnson DT. Growth and solvent production by *Clostridium pasteurianum* ATCC<sup>®</sup> 6013<sup>™</sup> utilizing biodiesel-derived crude glycerol as the sole carbon source. *Environ Prog Sustain Energy*. **28**: 1, 100–10 (2009).
13. Venkataramanan KP, Boatman JJ, Kurniawan Y, Taconi K a., Bothun GD, Scholz C. Impact of impurities in biodiesel-derived crude glycerol on the fermentation by *Clostridium pasteurianum* ATCC 6013. *Appl Microbiol Biotechnol*. **93**: 3, 1325–35 (2012).
14. Sarma SJ, Brar SK, Le Bihan Y, Buelna G, Soccol CR. Mitigation of the inhibitory effect of soap by magnesium salt treatment of crude glycerol - A novel approach for enhanced biohydrogen production from the biodiesel industry waste. *Bioresour Technol*. Elsevier Ltd, **151**: 49–53 (2014).
15. Salakkam A, Webb C. The inhibition effect of methanol, as a component of crude glycerol, on the growth rate of *Cupriavidus necator* and other micro-organisms. *Biochem Eng J*. Elsevier B.V., **98**: 84–90 (2015).

- Accepted Article
16. Chatzifragkou A, Papanikolaou S. Effect of impurities in biodiesel-derived waste glycerol on the performance and feasibility of biotechnological processes. *Appl Microbiol Biotechnol.* **95**: 1, 13–27 (2012).
  17. Thompson JC, He BB. Characterization of crude glycerol from biodiesel production from multiple feedstocks. *Appl Eng Agric.* **22**: 2, 261–5 (2006).
  18. Varrone C, Heggeset TMB, Le SB, Haugen T, Markussen S, Skiadas I V, et al. Comparison of Different Strategies for Selection/Adaptation of Mixed Microbial Cultures Able to Ferment Crude Glycerol Derived from Second-Generation Biodiesel. *Biomed Res Int.* HINDAWI PUBLISHING CORP, **2015**: (2015).
  19. Manosak R, Limpattayanate S, Hunsom M. Sequential-refining of crude glycerol derived from waste used-oil methyl ester plant via a combined process of chemical and adsorption. *Fuel Process Technol.* Elsevier B.V., **92**: 1, 92–9 (2011).
  20. Carmona M, Lech A, de Lucas A, Pérez A, Rodriguez JF. Purification of glycerol/water solutions from biodiesel synthesis by ion exchange: Sodium and chloride removal. Part II. *J Chem Technol Biotechnol.* **84**: 8, 1130–5 (2009).
  21. Anand P, Saxena RK. A comparative study of solvent-assisted pretreatment of biodiesel derived crude glycerol on growth and 1,3-propanediol production from *Citrobacter freundii*. *N Biotechnol.* **29**: 2, 199–205 (2012).
  22. Biebl H. Fermentation of glycerol by *Clostridium pasteurianum*-batch and continuous culture studies. *J Ind Microbiol Biotechnol.* **27**: 1, 18–26 (2001).
  23. Sarchami T, Johnson E, Rehmann L. Optimization of fermentation condition favoring butanol production from glycerol by *Clostridium pasteurianum* DSM 525. *Bioresour*



- Technol.* Elsevier Ltd, **208**: 73–80 (2016).
24. Sabra W, Groeger C, Sharma PN, Zeng AP. Improved n-butanol production by a non-acetone producing *Clostridium pasteurianum* DSMZ 525 in mixed substrate fermentation. *Appl Microbiol Biotechnol.* **98**: 9, 4267–76 (2014).
  25. Knoshaug EP, Zhang M. Butanol tolerance in a selection of microorganisms. *Appl Biochem Biotechnol.* **153**: 1–3, 13–20 (2009).
  26. Hviid A-MM, Jensen PR, Kilstrup M. Butanol is cytotoxic to *Lactococcus lactis* while ethanol and hexanol are cytostatic. *Microbiology.* 453–61 (2017).
  27. Wang YF, Tian J, Ji ZH, Song MY, Li H. Intracellular metabolic changes of *Clostridium acetobutylicum* and promotion to butanol tolerance during biobutanol fermentation. *Int J Biochem Cell Biol.* Elsevier Ltd, **78**: 297–306 (2016).
  28. Venkataramanan KP, Kurniawan Y, Boatman JJ, Haynes CH, Taconi K a., Martin L, et al. Homeoviscous response of *Clostridium pasteurianum* to butanol toxicity during glycerol fermentation. *J Biotechnol.* Elsevier B.V., **179**: 1, 8–14 (2014).
  29. Mayank R, Ranjan A, Moholkar VS. Mathematical models of ABE fermentation: review and analysis. *Crit Rev Biotechnol* [Internet]. **33**: 4, 419–47 (2013). Available from: <http://www.tandfonline.com/doi/full/10.3109/07388551.2012.726208>
  30. Zhang Q, Wu D, Lin Y, Wang X, Kong H, Tanaka S. Substrate and product inhibition on yeast performance in ethanol fermentation. *Energy and Fuels.* **29**: 2, 1019–27 (2015).
  31. Georgieva TI, Skiadas I V., Ahring BK. Effect of temperature on ethanol tolerance of a thermophilic anaerobic ethanol producer *Thermoanaerobacter* A10: Modeling and

- simulation. *Biotechnol Bioeng.* **98**: 6, 1161–70 (2007).
32. Ordoñez MC, Raftery JP, Jaladi T, Chen X, Kao K, Karim MN. Modelling of batch kinetics of aerobic carotenoid production using *Saccharomyces cerevisiae*. *Biochem Eng J.* **114**: 226–36 (2016).
33. Domínguez H, Nuñez MJ, Lema JM. Determination of Kinetic Parameters of Fermentation Processes by a Continuous Unsteady-State Method: Application to the Alcoholic Fermentation of D-Xylose by *Pichia stipitis*. *Biotechnol Bioeng.* **41**: 1129–32 (1993).
34. Kalfas H, Skiadas I V, Gavala HN, Stamatelatou K, Lyberatos G. Application of ADM1 for the simulation of anaerobic digestion of olive pulp under mesophilic and thermophilic conditions. *Water Sci Technol.* **54**: 4, 149–56 (2006).
35. Jurado E, Antonopoulou G, Lyberatos G, Gavala HN, Skiadas IV. Continuous anaerobic digestion of swine manure: ADM1-based modelling and effect of addition of swine manure fibers pretreated with aqueous ammonia soaking. *Appl Energy.* **172**: (2016).
36. Dabrock B, Bahl H, Gottschalk G. Parameters affecting solvent production by *Clostridium pasteurianum*. *Appl Environ Microbiol.* **58**: 4, 1233–9 (1992).
37. APHA. American Public Health Association. Standard methods for examination of water and wastewater, 21st edn. APHA, AWWA, WPCF, Washington. (2005).
38. Rittmann BE, McCarty PL. Environmental Biotechnology: Principles and Applications. McGraw-Hill Series in Water Resources and Environmental Engineering. 463 p.(2001).

39. Reichert P. Aquasim 2.0 - Computer Program for the Identification and Simulation of Aquatic Systems. EAWAG. Dübendorf, Switzerland, (1998).
40. Groeger C, Wang W, Sabra W, Utesch T, Zeng A-P. Metabolic and proteomic analyses of product selectivity and redox regulation in *Clostridium pasteurianum* grown on glycerol under varied iron availability. *Microb Cell Fact.* BioMed Central, **16**: 1, 64 (2017).
41. Zhu C, Fang B, Wang S. Effects of culture conditions on the kinetic behavior of 1,3-propanediol fermentation by *Clostridium butyricum* with a kinetic model. *Bioresour Technol.* Elsevier Ltd, **212**: 130–7 (2016).
42. Lo Y-C, Chen X-J, Huang C-Y, Yuan Y-J, Chang J-S. Dark fermentative hydrogen production with crude glycerol from biodiesel industry using indigenous hydrogen-producing bacteria. *Int J Hydrogen Energy.* Elsevier Ltd, **38**: 35, 15815–22 (2013).
43. Costa J, Moreira A. Growth inhibition kinetics for the acetone-butanol fermentation. *ACS Symp Ser.* **207**: 207, 501–12 (1983).

## List of Tables captions

**Table 1.** The values of the kinetic parameters together with the estimated standard deviation

**Table 2.** Correlation matrix of the kinetic constants

**Table 3.** Stoichiometric coefficients for the overall conversion of glycerol to products and cells applied for *C. pasteurianum* growth for the batch fermentation and the different steady states with increasing influent butanol concentration.

## List of Figures captions

**Figure 1.** Comparison of glycerol consumption (A) and cell growth (B) between hexane treated (HT), non-hexane treated and pure glycerol.

**Figure 2.** Calibration curve for calculating the mass of microbial cells.

**Figure 3.** Experimental and predicted by the model profile of glycerol concentration during the CSTR (A and B) and batch (C) fermentations.

**Figure 4.** Experimental and predicted by the model profile of butanol concentration during the CSTR (A) and batch (B) fermentations.

**Figure 5.** Experimental and predicted by the model profile of cells concentration during the CSTR (A) and batch (B) fermentations.

**Figure 6.** Sensitivity functions of the model state variables (glycerol, butanol and cells concentration) with respect to inhibition constant  $K_I$  during the CSTR (A) and batch (B) fermentations.

**Table 1.** The values of the kinetic parameters together with the estimated standard deviation

<b>Kinetic constant</b>	<b>Estimated value</b>	<b>Estimated standard deviation</b>
$\mu_{\max}$ , h <sup>-1</sup>	0.60	± 0.08
$K_S$ , g/L	1.13	± 0.37
$K_I$ , g/L	7.64	± 1.91
$K_d$ , h <sup>-1</sup>	0.007	± 0.002

**Table 2.** Correlation matrix of the kinetic constants

	$K_d$	$K_I$	$K_S$	$\mu_{\max}$
$K_d$	1	0.04	-0.262	-0.136
$K_I$	0.050	1	0.573	-0.424
$K_S$	-0.262	0.57	1	0.427
$\mu_{\max}$	-0.136	-0.42	0.427	1

**Table 3.** Stoichiometric coefficients for the overall conversion of glycerol to products and cells applied for *C. pasteurianum* growth for the batch fermentation and the different steady states with increasing influent butanol concentration.

Steady state	Reactants			Products					Electron fractions							
	C <sub>3</sub> H <sub>8</sub> O <sub>3</sub> glycerol	HCO <sub>3</sub> <sup>-</sup>	NH <sub>4</sub> <sup>+</sup>	C <sub>2</sub> H <sub>5</sub> OH Ethanol	C <sub>2</sub> H <sub>4</sub> O <sub>2</sub> Acetate	C <sub>3</sub> H <sub>8</sub> O <sub>2</sub> 1,3-PDO	C <sub>4</sub> H <sub>10</sub> O Butanol	C <sub>4</sub> H <sub>8</sub> O <sub>2</sub> Butyrate	H <sub>2</sub>	CO <sub>2</sub>	H <sub>2</sub> O	C <sub>5</sub> H <sub>7</sub> O <sub>2</sub> N Cells	$f_e$ Products	$f_s$ Cells, theor.	$f_{s,exp}$ Cells, exp.	$f_m$ Maintenance
1 <sup>st</sup>	1	0.193	0.193	0.219	0.020	0.145	0.201	0.006	0.597	0.708	0.979	0.138	0.803	0.197	0.102	0.095
2 <sup>nd</sup>	1	0.145	0.145	0.286	0.018	0.143	0.207	0.009	0.648	0.761	0.747	0.084	0.879	0.121	0.098	0.022
3 <sup>rd</sup>	1	0.169	0.169	0.223	0.019	0.176	0.192	0.014	0.631	0.723	0.851	0.111	0.842	0.158	0.087	0.071
4 <sup>th</sup>	1	0.171	0.171	0.262	0.017	0.160	0.188	0.007	0.617	0.727	0.860	0.114	0.837	0.163	0.088	0.075
5 <sup>th</sup>	1	0.211	0.211	0.204	0.016	0.182	0.171	0.004	0.615	0.695	0.998	0.154	0.781	0.219	0.085	0.135
batch	1	0.107	0.107	0.150	0.047	0.126	0.283	0.019	0.246	0.591	1.155	0.107	0.846	0.154	0.094	0.059



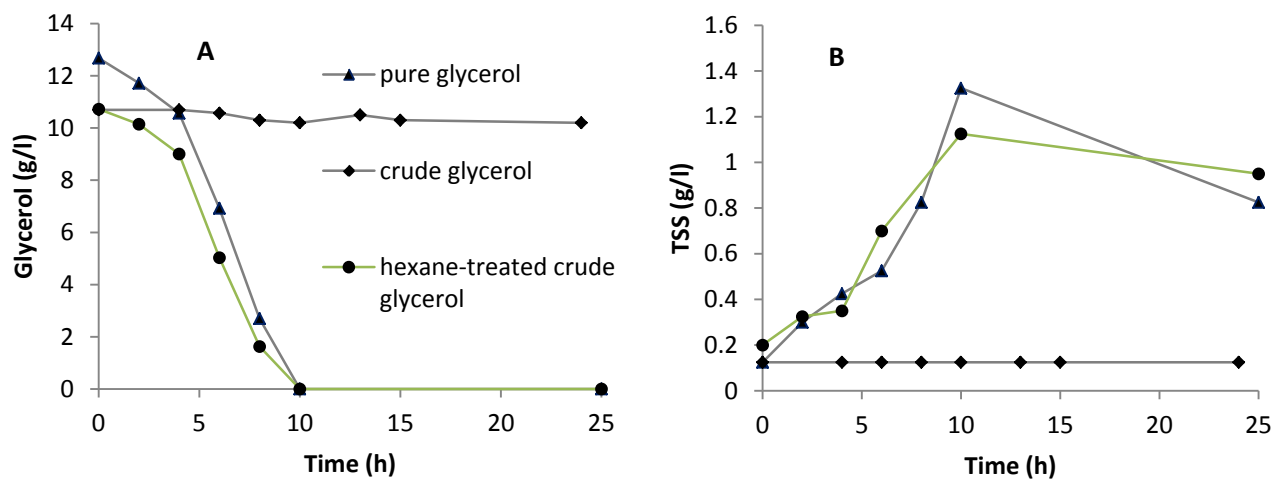


**Figure 1.** Comparison of glycerol consumption (A) and cell growth (B) between hexane treated (HT), non-hexane treated and pure glycerol.

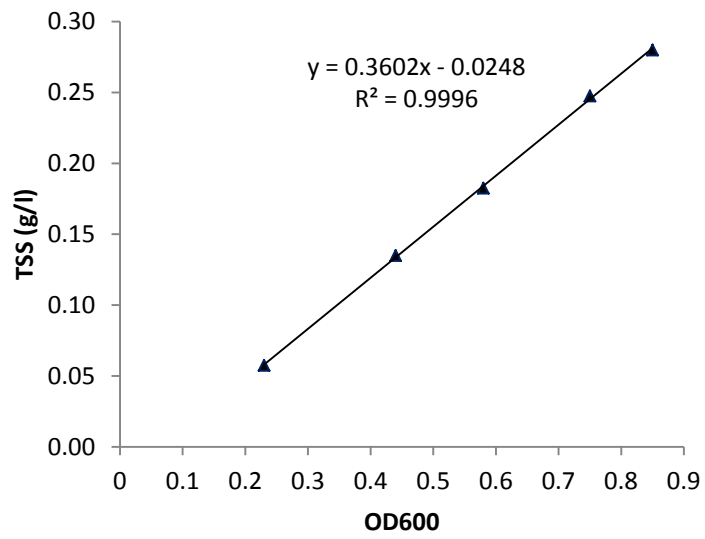


**Figure 2.** Calibration curve for calculating the mass of microbial cells.

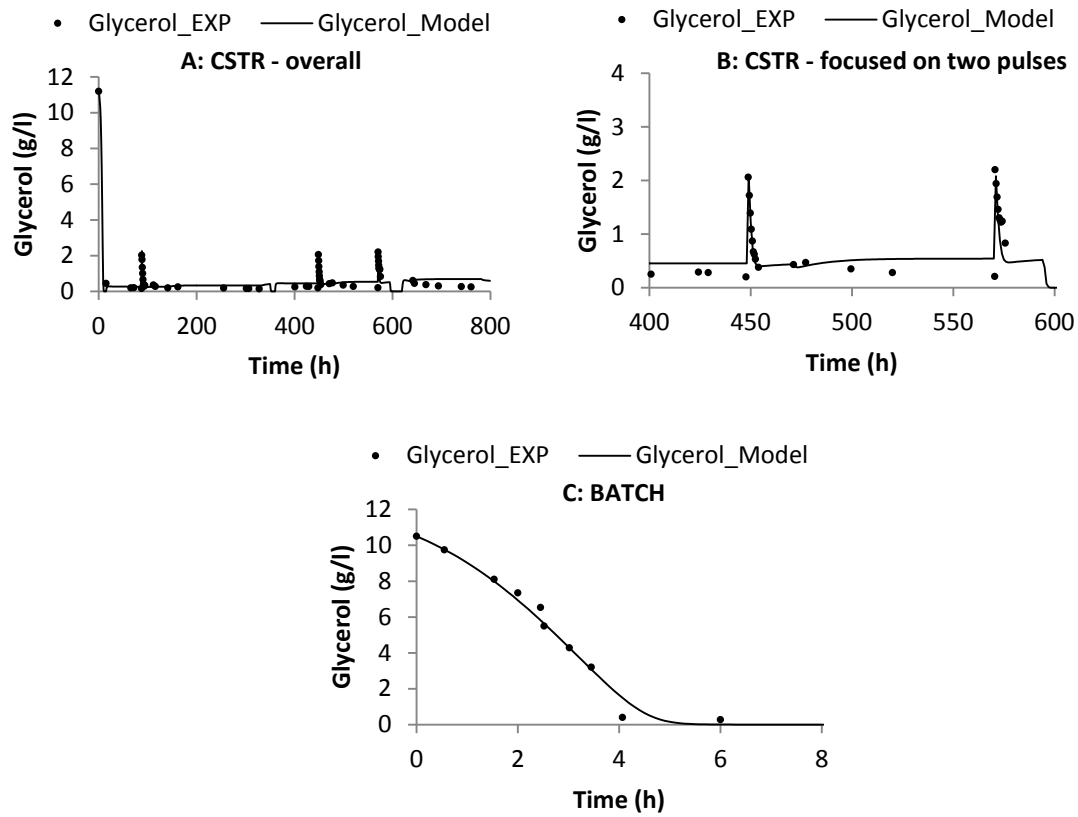


**Figure 3.** Experimental and predicted by the model profile of glycerol concentration during the CSTR (A and B) and batch (C) fermentations.

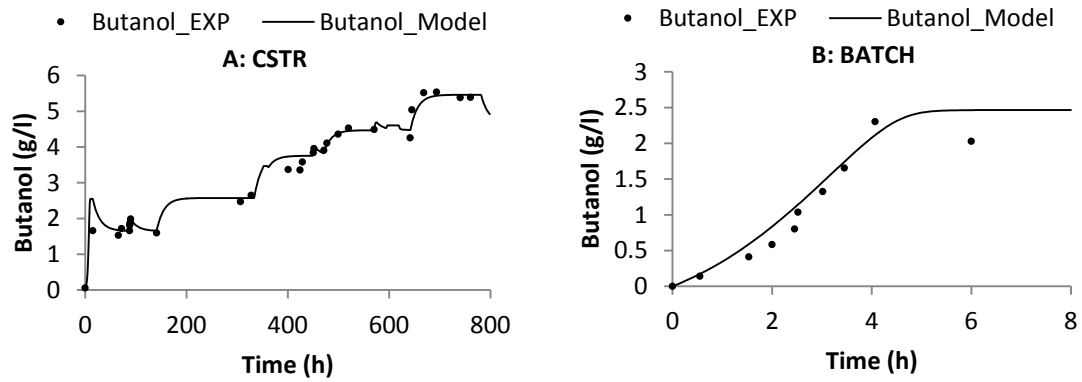


**Figure 4.** Experimental and predicted by the model profile of butanol concentration during the CSTR (A) and batch (B) fermentations.

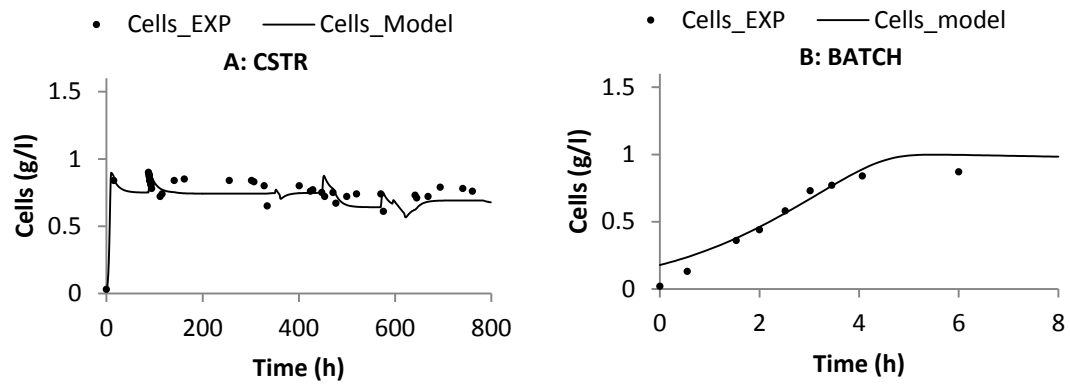


**Figure 5.** Experimental and predicted by the model profile of cells concentration during the CSTR (A) and batch (B) fermentations.

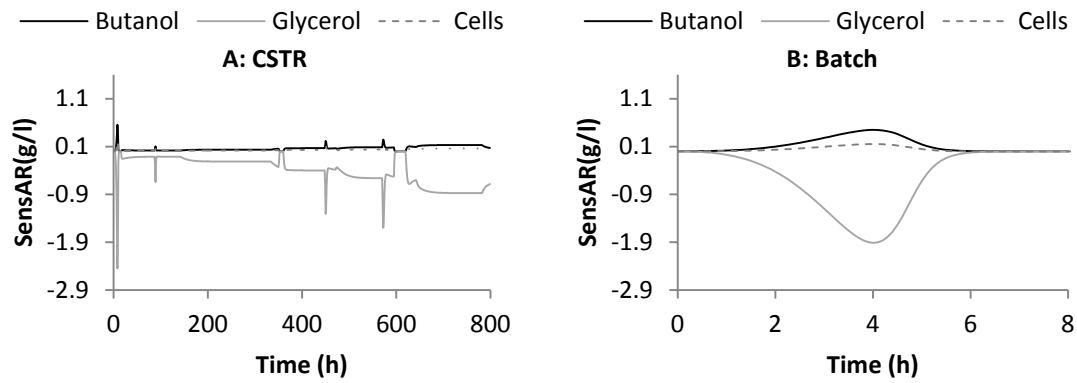


**Figure 6.** Sensitivity functions of the model state variables (glycerol, butanol and cells concentration) with respect to inhibition constant  $K_I$  during the CSTR (A) and batch (B) fermentations.